CIPM MRA
Comparison reports

BIPM.EM-K10.a.b.c.d (CENAM 2025)

DC and AC voltage, Josephson standards

KEY COMPARISON

Any further distribution of this Report must be cited as:
S. Solve *et al* 2026 *CIPM MRA Comparison reports* **01006**

https://doi.org/10.59161/QGWE3582

DC and AC voltage comparison of the Josephson Voltage Standards of the CENAM and the BIPM

(part of the ongoing BIPM key comparison BIPM.EM-K10.a, .b, .c and .d)

S. Solve[1], R. Chayramy[1], M. Stock[1], J. Medina Mejía[2] and R. Gutiérrez Gómez[2]

[1]Bureau International des Poids et Mesures
F- 92312 Sèvres Cedex, France

[2]Centro Nacional de Metrología
km 4.5 Carretera a Los Cués,
El Marqués, Querétaro, México

Abstract. A comparison of the DC primary voltage realisation and a comparison of the root mean square (RMS) amplitude of a sinewave (AC signal) were performed between the *Bureau International des Poids et Mesures* (BIPM) and the *Centro Nacional de Metrología* (CENAM) in the CENAM laboratory in Querétaro, Mexico in August 2025. For the DC comparison, the BIPM transportable Programmable Josephson Voltage Standard (BIPM-PJVS) was directly compared to the CENAM Programmable Josephson Voltage Standard (CENAM-PJVS) by means of an analog nanovoltmeter at 1 V and 10 V. For the AC comparison, the AC signal generated by a BIPM generator was measured alternatively by the BIPM-PJVS and the CENAM-PJVS. The comparison was carried out at RMS voltages of 0.75 V and 7 V at different frequencies in the range from 62.5 Hz to 1250 Hz. This is the second key comparison since the extension of the BIPM.EM-K10 comparison protocol[1] to AC measurements, endorsed by the Consultative Committee for Electricity and Magnetism (CCEM) in June 2022. The relative agreement between the two quantum voltage standards was within 3.6 parts in 10^{11} and 5.7 parts in 10^{10} at 10 V DC and 1 V DC, respectively. The final results of the AC measurements were also in good agreement, to within a few parts in 10^{7} at 0.75 V RMS for several frequencies and a few parts in 10^{9} at 7 V RMS at 62.5 Hz, respectively.

1. Introduction

Within the framework of *Mutual Recognition Arrangement of the Comité International des Poids et Mesures* (CIPM MRA) key comparisons, the *Bureau International des Poids et Mesures* (BIPM) and the *Centro Nacional de Metrología* (CENAM) performed an on-site comparison of the realisation of the volt and a comparison of measurements of the root mean square (RMS) amplitude of a sinewave (AC signal) generated by a BIPM generator operated as a transfer standard. The comparison was carried out at CENAM in Querétaro, Mexico, from 5 August to 26 August 2025. This exercise is the second of this type and follows the new protocol for BIPM.EM-K10 extended to AC voltages which was endorsed by the Consultative Committee for Electricity and Magnetism (CCEM) in June 2022 [1]. At DC, the two quantum voltage standards were compared directly by means of an analog nanovoltmeter. At AC, an accurate AC source, designed as the BIPM transfer standard, was measured alternatively by the BIPM transportable Josephson Voltage Standard (BIPM-PJVS) and associated measurement setup and that of the CENAM (CENAM-PJVS), using the differential sampling technique [2-10].

[1] In addition to DC comparisons: .a for 1 V and .b for 10 V, BIPM.EM-K10 offers 2 new extensions: .c for 0.75 V RMS and .d for 7 V RMS.

The present comparison followed the option II (DC) and the option IV (AC) technical rules of the BIPM.EM-K10 comparison protocol for the following voltages:

- BIPM.EM-K10.a: 1 V DC;
- BIPM.EM-K10.b: 10 V DC;
- BIPM.EM-K10.c: 0.75 V RMS AC;
- BIPM.EM-K10.d: 7 V RMS AC.

This article describes the technical details and the results of the experiments carried out during the comparison.

2. Comparison equipment

2.1 The BIPM DC voltage standard and AC quantum voltmeter

The BIPM traveling quantum voltage standard is a Programmable Josephson Voltage Standard (BIPM-PJVS), which is composed of a cryoprobe that carries a liquid helium version of the 2 V or 10 V SNS NIST programmable array [11-13]. In the present exercise, only the 10 V array was operated. The voltage across the array is controlled by a dedicated microwave source and a dedicated bias source. The array must be cooled down in a bath of liquid He the temperature of which is determined by the atmospheric pressure. Since the CENAM laboratory is located at an altitude of 1980 m, the liquid He temperature was lower than 4 K leading to excellent working conditions (the DC flatspot was increased by about 40 % reaching 1.8 mA while typically at the level of 1.3 mA in the BIPM laboratory). The PJVS was operated with the NIST bias source (JVS-650) and associated software (*iPJVS Core* 2021-v1208) at all voltages. The BIPM traveling quantum voltage standard is flexible and can be modified to limit the errors, when identified, introduced by the participant's electromagnetic environment and possible systematic errors and noise due to grounding effects and/or AC capacitive coupling effects. The BIPM-PJVS is electrically floating with no connection to earth potential, but its low potential side can be grounded whenever necessary. The series resistance of each of the precision measurement leads is 2.5 Ω, and their leakage resistance to earth is 80 GΩ. These values are checked on-site using a dedicated feature of the *iPJVS Core* software. However, the AC component, i.e. capacitive component of the leakage impedance cannot be measured easily. This component increases the leakage error as the frequency of the measured signal rises. The value of the thermal electromotive forces (EMFs) measured at the level of the output connection (at the laboratory temperature) is in the range 600-900 nV.

For the comparison measurement the BIPM used the following equipment:

- At DC: an EM-N11 analog nanovoltmeter, its associated reversal switch and the control software to measure the voltage difference between the two quantum voltage standards.

- At AC: a PXI-NI-5922[2] , a Fluke 8588A, or Agilent 3458A (only for 62.5 Hz) sampler and associated control software to measure the RMS value of sinewaves generated by the BIPM transfer standard consisting of a Signal Waveform Generator (SWG) generator and filter [1,14] using the differential sampling technique.

For the AC voltage comparison, the setup is flexible and allows a large number of possibilities for differential sampling, among which the principal ones are:

- 2 V array instead of 10 V array to limit the number of cells constituting the array and corresponding leakage paths to ground. This possibility was not used at CENAM.
- Both PJVS systems can use a single 10 MHz reference for timing and RF bias, which was applied using the reference provided by CENAM.
- The stepwise approximated sinewave of the BIPM-PJVS was synchronized to the *Sync Out* Signal of the AC source SWG (voltage transfer standard). This signal was fed as the external clock signal to the PJVS bias source timing board.
- The BIPM differential sampling setup can operate three different samplers. During this comparison all of them were tested to check for the measurement conditions: at 62.5 Hz, the agreement of the results obtained with the three samplers gives a strong confidence that the measurement setup offers reproducible conditions (cf. Figure 9). Most of the results were obtained with the NI PXI-5922. The sampler is inserted into a NI-PXI 1031DC chassis powered by an isolated supply and PC-controlled via an optical link.
- The BIPM can operate different software. The software developed in collaboration with KRISS was used for all AC measurements.
- The SWG BIPM transfer standard and associated filter were operated on batteries and an external battery pack connected to each device ensured long-term operation.

2.2 The CENAM AC quantum voltmeter

[2] **DISCLAIMER**

Certain commercial equipment, instruments or materials are identified in this paper in order to adequately specify the environmental and experimental procedures. Such identification does not imply recommendation or endorsement by the BIPM or CENAM, nor does it imply that the materials or equipment identified are necessarily the best available for the purpose.

The quantum voltage standard developed at CENAM is a Programmable Josephson Voltage Standard (PJVS), comprising a hybrid configuration of commercial instruments and in-house technological developments. The system employs a 10 V SNS array from NIST, with the voltage across the array controlled by a dedicated microwave source and a bias source designed at CENAM.

The array is cooled using a cryocooler-based system, which maintains an operating temperature of 4.2 K, providing the optimal conditions for stable Josephson operation. Through optimization of temperature, microwave frequency, and power, a Quantum Locking Range (QLR) of 1.6 mA is achieved, corresponding to the point of maximum quantization stability.

The PJVS-CENAM operates a bias source and control software developed at CENAM [15-16], supporting both DC and AC applications. Bias currents are supplied by independent, battery-powered current sources for each subarray, ensuring floating operation without ground connection. Synchronization and triggering are fully optically isolated, including communication with the data acquisition system.

Electrical characteristics of the system include a series resistance of 1.3 Ω for the precision measurement leads and a leakage resistance to ground of 23 GΩ, determined using the NIST method [17]. The thermal electromotive forces (EMFs) at the output terminals, measured at room temperature, range from 600 to 900 nV.

For AC measurements, the PJVS-CENAM employs a differential sampling configuration using high-precision digitizers, specifically the Agilent 3458A and Fluke 8588A. In this comparison, the Fluke 8588A was selected due to its 3 MHz analog bandwidth, enabling measurements in the kilohertz range used in the experiment. The stepwise-approximated sinusoidal waveform generated by the PJVS-CENAM provides the zero-crossing synchronization signal and can also be synchronized to an optically isolated external clock.

The CENAM software manages signal acquisition, waveform reconstruction, and analysis at various voltages and frequencies. After differential reconstruction, the RMS voltage is obtained using a three-parameter fitting algorithm. During the comparison, phase adjustment was performed by evaluating the differences between the reference and measured waveforms, determining the optimal phase shift to minimize deviations, and applying the corresponding correction to the BIPM's SWG transfer standard to achieve minimal discrepancies.

3. DC Voltage Comparison procedure - Option II

3.1 Introduction

The option II comparison protocol for DC direct comparison has been designed to achieve the lowest Type A uncertainty on the voltage difference between the participants using an analog nanovoltmeter EM-N11 which offers a lower internal noise than a digital nanovoltmeter. However, the Option II protocol is always started with a digital nanovoltmeter to investigate the noise level on the PJVS voltages in particular during the process of finding the best grounding configuration of the two connected setups. If the Type A uncertainty of the series of points reaches the noise floor of the digital detector, it is worth to switch to the analog detector. In the present case, a Type A uncertainty of 3 nV was quickly reached using an HP3440A digital nanovoltmeter and therefore, the analog nanovoltmeter was implemented [15-16].

3.2 Measurement precautions and improvements

After the BIPM-PJVS was set up, the array of Josephson junctions was checked for trapped flux.
Before we present the results achieved, a few important statements should be made about the measurement setup:

1) Both Josephson systems were connected to the same power strip. Since the mains voltage is 120 V, a special arrangement was made on the main panel of the CENAM power strip to power the BIPM equipment on 220 V. This configuration utilized a built-in feature that allows for a higher output amplitude through an internal switch, in combination with the power amplifier. This setup was used to supply the voltage on the phase used by the BIPM within the laboratory.

2) The earthing point, which was used in a star configuration for all earthing, was located on the shield of the CENAM cryo-cooler.

3) After each measurement sequence in a specific polarity, both array voltages were set to zero, the measurement line was opened and the arrays were set to the opposite polarity voltage. The circuit was closed and the next polarity measurement could be started.

3.3 Measurement setup

The measurement loop operated for the option II comparison is shown in Figure 1.

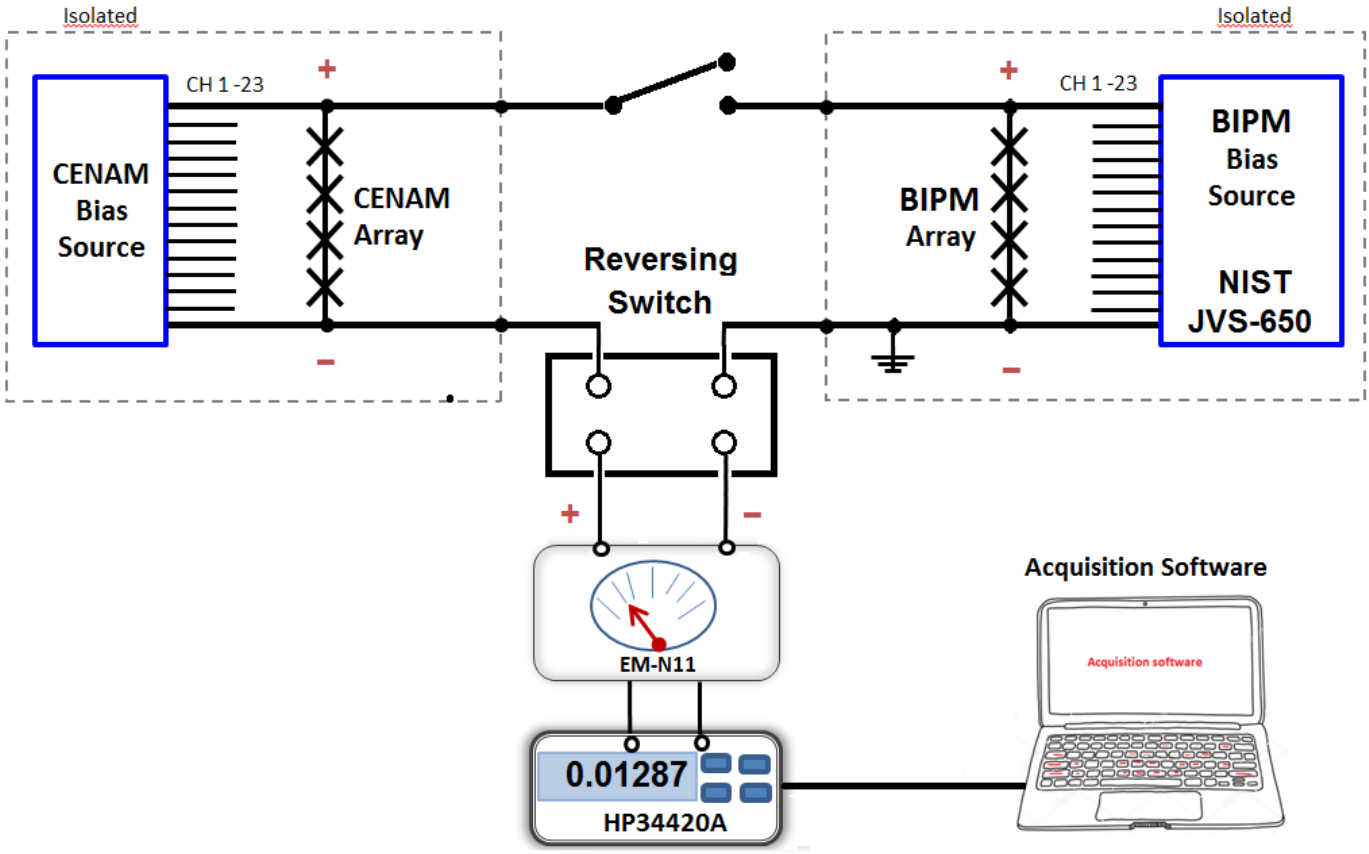

Fig. 1: Measurement setup used for the Option II (1 V and 10 V DC). The switch which reverses the nanovoltmeter input also has an "open position" (represented at the top of the figure for clarity) that was used before each polarity reversal in order to avoid trapping flux.

3.4 Measurement procedure

To obtain a single measurement point, the polarity reversals of the voltage standards are performed with a low thermal electromotive forces (EMFs) switch in the following sequence:

1- The CENAM array and the BIPM array are set in their positive polarity, connected in series opposition and the detector data reading sequence starts;
2- The polarity of the detector is reversed and a reading sequence is carried out. The number of measurements is twice the number acquired in step 1;

3- The CENAM and the BIPM arrays remain in their positive polarity and the detector is reversed in order to match exactly the configuration of step 1; the reading sequence starts again;
4- The CENAM and the BIPM arrays are set in their negative polarity, connected in series opposition and the detector data reading sequence starts;
5- The polarity of the detector is reversed and a reading sequence is carried out. The number of measurements is twice the number acquired in step 4;
6- The CENAM and the BIPM arrays remain in their negative polarity and the detector is reversed in order to match exactly the configuration of step 4; the reading sequence starts again;

Each “reading sequence” step starts with the acquisition of 50 readings for which the standard deviation, σ_p is calculated. This preliminary series is then followed by 100 new readings and each of them must stay within four times σ_p of the mean value of the preliminary series. If this is not the case, the software warns the operator with a beep. If 10 beeps occur in a row, the operator must restart the “reading sequence” step in progress.

Remark 1: During the detector reversed position acquisition (steps 2 and 5), a total of 200 readings are monitored in such a way that for the calculation of a measurement point, the total aperture times in the forward and reverse position of the detector are the same.

Remark 2: Prior to the polarity reversal of the arrays, the measurement circuit is opened using a dedicated switch in order to avoid possible flux trapping in the arrays within the reversal process.

3.5 Uncertainties

The Type A uncertainty is calculated as the standard deviation of the mean of the measured differences between the CENAM and the BIPM voltages. One series of 16 individual points was performed at the 1 V level. Three different series for a total of 27 individual points were performed at the 10 V level. The relative Type B components for both voltage levels are presented in the following table (Table 1) and an explanation on the calculation of each component is also provided.

	Type	Relative uncertainty	
		BIPM	**CENAM**
Frequency offset (A)	B	3.2×10^{-12}	3.2×10^{-13}
Leakage resistance (B)	B	1.8×10^{-11}	3.3×10^{-11}
Detector (C)	B	2.0×10^{-11}	
Total (RSS)	B	2.7×10^{-11}	3.3×10^{-11}

Table 1: Estimated Type B relative standard uncertainty components.

(A) As both systems were referred to the same 10 MHz frequency reference, only a Type B uncertainty for the frequency is included. The 10 MHz signal used as the frequency reference for the comparison was distributed from an HP 5071A Cs primary frequency standard, which was previously compared against the main atomic clocks from the time and frequency laboratory of CENAM.

The BIPM PJVS RF synthesiser frequency has an accuracy better than 0.01 Hz. We degrade this accuracy by 10 and apply a rectangular statistical distribution to the value. The relative uncertainty for the offset of the frequency can be calculated from the formula: $u_f = (0.1/\sqrt{3}) \times (1/18) \times 10^{-9} = 3.2 \times 10^{-12}$.

CENAM's microwave synthesizer is an Agilent E8257D whose frequency synthesis is better than 0.01 Hz. During the DC voltage comparison, the Josephson array was fed with a signal with a frequency of 18.24 GHz. We apply a rectangular statistical distribution to the value, therefore the relative uncertainty for the offset of the frequency is: $u_f = (0.01/\sqrt{3}) \times (1/18.24) \times 10^{-9} = 3.2 \times 10^{-13}$.

(B) If a rectangular statistical distribution is assumed then the relative uncertainty contribution of the leakage resistance R_L to the BIPM uncertainty can be calculated as: $u_L = (1/\sqrt{3}) \times (r / R_L)$, where $r = 2.5\ \Omega$ is the series resistance of the measurement leads and 80 GΩ the isolation resistance. For CENAM, the related variables were measured to be $r = 1.3\ \Omega$ and $R_L = 23$ GΩ. The isolation resistance value includes all the cables from the PJVS to the DVM.

(C) A EM N11 served as the null detector on the 10 µV range at 10 V and 3 µV at 1 V. Although the two PJVS were exactly set to 10 V, the maximum remaining thermal EMFs between the two standards, of amplitude 700 nV were measured by the nanovoltmeter. The gain correction was not measured since it is insignificant to be applied to the readings. The uncertainty on the gain is about 5×10^{-4} according to our experience with this type of nanovoltmeter [16]. We apply this uncertainty to the maximum measured voltage considering a rectangular statistical distribution: the absolute standard uncertainty of the detector can then be calculated as follows: $5 \times 10^{-4} \times 700$ nV/ $\sqrt{3}$ = 2.02×10^{-10} V. So, the relative uncertainty is $u_d = 2 \times 10^{-11}$.

4. Comparison results - Option II at the 1 V and 10 V DC level

4.1 Measurements at 1 V

The results obtained at the 1 V level are presented on the following graph (Fig. 2) where the uncertainty bars represent the Type A uncertainty only (0.85 nV). The straight line represents the mean value (-0.57 nV).

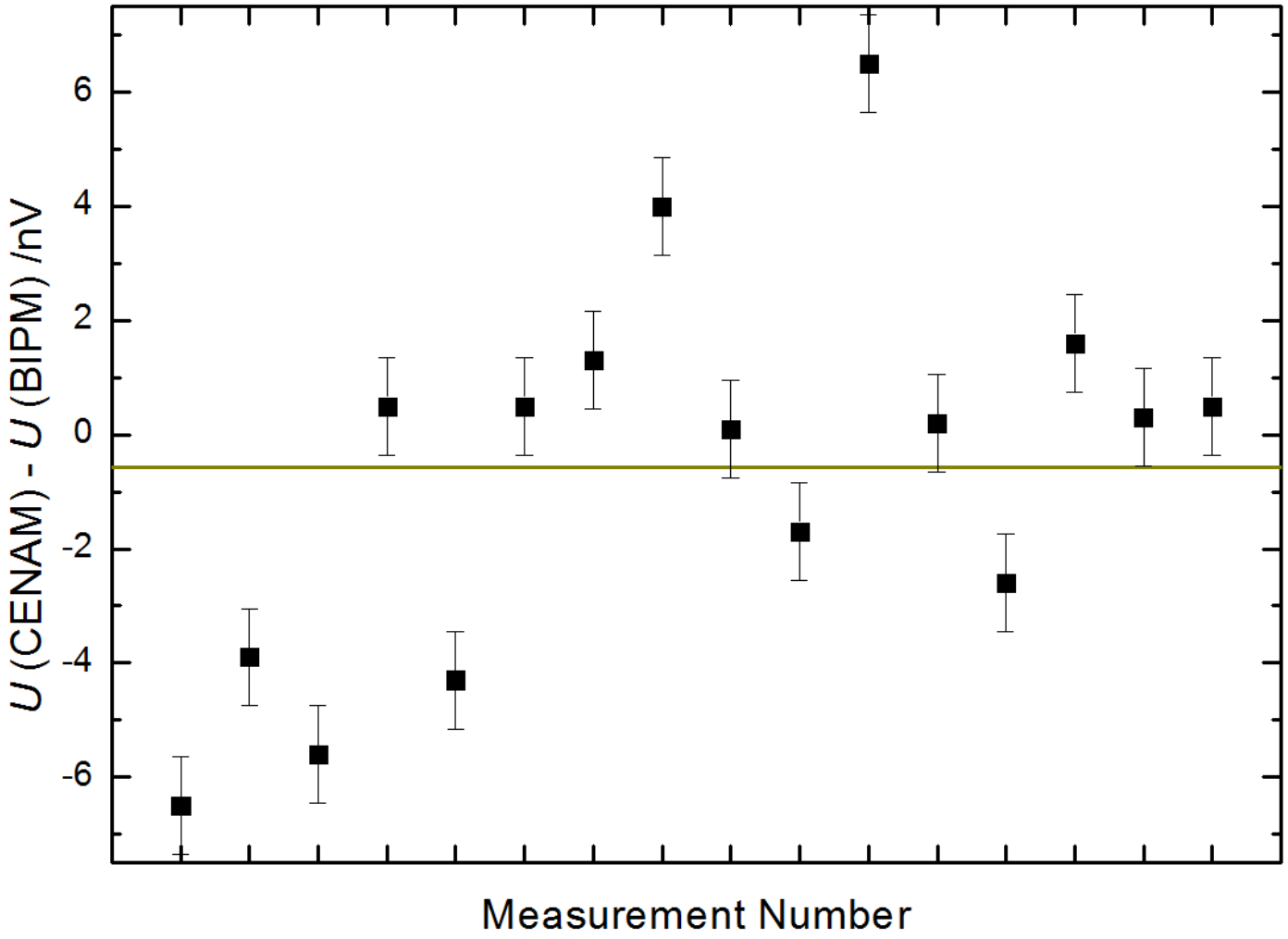

Fig. 2: Individual results obtained for the final result of the Option II comparison protocol at the 1 V level using an analog nanovoltmeter within the same measurement conditions. The uncertainty bars represent the Type A standard uncertainty.

The result obtained is expressed as the relative difference between the values attributed to the 1 V CENAM PJVS by the BIPM PJVS measurement set-up (U_{CENAM}) and the 1 V BIPM PJVS (U_{BIPM}):

$$(U_{CENAM} - U_{BIPM}) / U_{BIPM} = -5.7 \times 10^{-10} \quad \text{and} \quad u_c / U_{BIPM} = 8.7 \times 10^{-10}$$

where u_c is the total combined standard uncertainty, and the relative Type A uncertainty is $u_A / U_{BIPM} = 8.5 \times 10^{-10}$.

4.2 Measurements at 10 V

The results obtained at the 10 V level are presented on the following graph (Fig. 3) where the uncertainty bars represent the Type A uncertainty only (0.68 nV). The straight line represents the mean value (+0.36 nV).

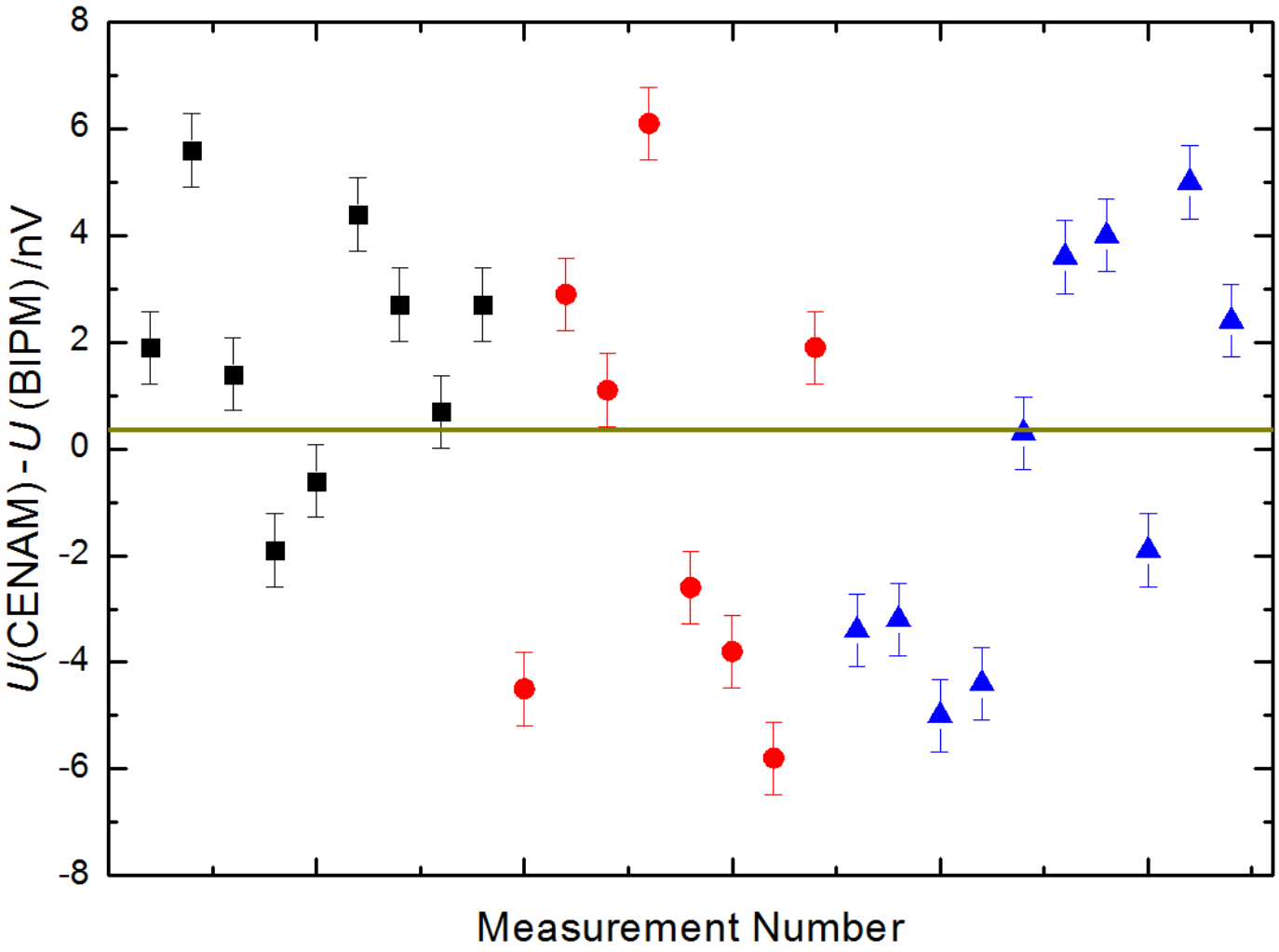

Fig. 3: Individual results obtained for the final result of the Option II comparison protocol at the 10 V level using an analog nanovoltmeter. The three series were performed within the same measurement conditions. The uncertainty bars represent the Type A standard uncertainty.

The result obtained is expressed as the relative difference between the values attributed to the 10 V CENAM PJVS by the BIPM PJVS measurement set-up (U_{CENAM}) and the 10 V BIPM PJVS (U_{BIPM}):

$$(U_{CENAM} - U_{BIPM}) / U_{BIPM} = +3.6 \times 10^{-11} \text{ and } u_c / U_{BIPM} = 8.0 \times 10^{-11}$$

where u_c is the total combined standard uncertainty, and the relative Type A uncertainty is $u_A / U_{BIPM} = 6.8 \times 10^{-11}$.

4. AC Voltage Comparison procedure - Option IV

4.1 Introduction

The option IV comparison protocol has been designed to achieve the lowest voltage difference and corresponding Type A uncertainty between the participants.

The 10 MHz reference signal distributed in the CENAM laboratory was used by both setups. In order to avoid any interference, the signal was decoupled between the two setups using isolation transformers.

In option IV, the transfer standard is an AC source and associated output filter provided by the BIPM (commercial AC source designed and assembled at CMI - Czech Metrology Institute) [14].

A computer-controlled switch (BNC connectors type) was installed on the BIPM transfer standard in order to easily switch its output between the BIPM measurement setup and the CENAM measurement setup and thereby to reduce the connection time to the minimum possible. Furthermore and more importantly, any physical manipulations and related possible changes (impedance adaption) between the two measurement setups are avoided.

The voltage difference between the two participants is evaluated from a series of individual measurements performed by each participant following an **ABBA** sequence, where **A** stands for the CENAM and **B** for the BIPM. A measurement point is derived from typically five individual measurements with each setup. More details on this measurement acquisition process are given in the next paragraph.

4.2 Measurement precautions and improvements

After the BIPM PJVS was set up, the array of Josephson junctions was checked for trapped flux.

Before carrying out the comparisons, the best grounding configuration was determined:

1) Both Josephson systems were connected to the same power strip even if they require different line voltages.

2) Choice of the Central Reference Point (see also 4.4): The earthing point, which was used in a star configuration for all earthing, was located on this power strip and more precisely on the chassis of the CENAM cryo-cooler.

3) This configuration provided the best results in the pilot studies. In the present comparison, it was also the case at CENAM for the best results achieved. However, within certain circumstances which were not clearly identified but probably coming from a change in the earthing potential of the CENAM mains, it was impossible to use it due to a large level of electrical noise brought to the BIPM system.

4.3 Measurement setup

The measurement loop operated for the option IV comparison is based on the synchronization of the two AC quantum voltmeters with the AC source. A schematic of the setup and the synchronization is shown in Fig. 4: The stepwise approximated sinewave of the BIPM-PJVS is synchronized to the *Sync Out* Signal of the AC source SWG. The sampler *Trig In* signal is produced by a function generator which is itself also triggered by the *Sync Out* Signal of the AC source SWG. The *Sync Out* signal of the AC source is of course in phase with the AC source signal, therefore the three components, AC source signal, PJVS approximated waveform and sampler windows, are aligned.

In the case of the CENAM setup, the alignment between the AC source and the stepwise approximated waveform was performed by directly measuring the phase difference between the two signals. The AC source signal was then shifted by the measured phase difference. The AC source phase is extremely stable and once this adjustment was applied, there was no need to update it during the measurement sequence.

Once the two systems had been synchronised with the SWG, the measurements of the output voltage of the SWG could be carried out in quick succession. An **ABBA** measurement took about 5 minutes and due to the fast switching between the two Josephson systems without the need for further adjustment steps, the drift of the AC source, although typically less than 1×10^{-7} V V^{-1} over 30 minutes, could be tracked very well. This reduced the Type A measurement uncertainty. Some examples of such measurement series are shown in the appendix.

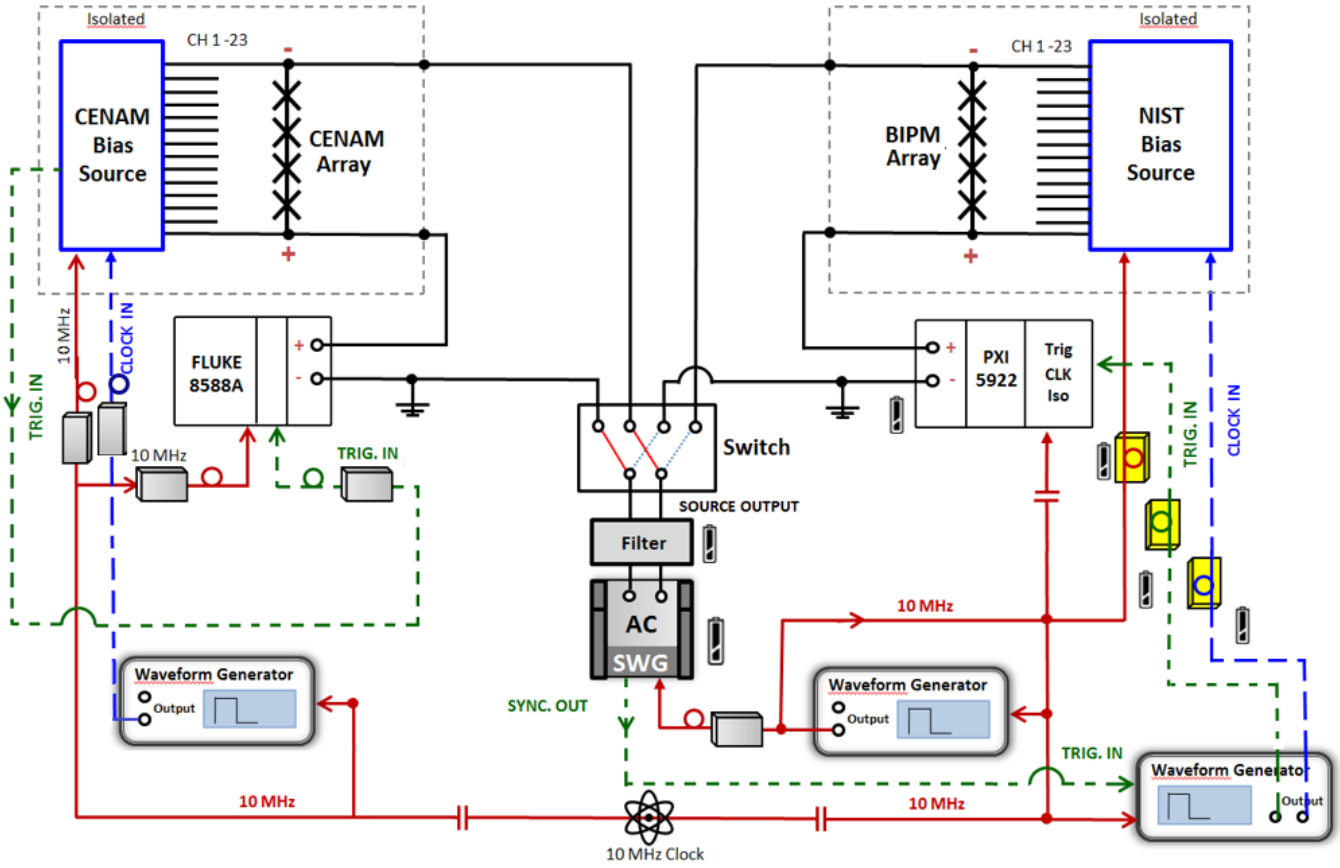

Fig. 4: Measurement setup used for the 0.75 V and 7 V RMS comparisons including the synchronization scheme. Red lines show 10 MHz distribution, green lines trigger connections and blue lines clock signal to the BIPM and CENAM PJVS. Optical isolators are indicated by loops on the connections.

4.4 Central Reference Point

The earthing concept is based on the optimised strategy developed in the pilot studies. It consists of a central potential reference point: Earth of the CENAM laboratory taken from the shield of the CENAM cryocooler, designed as “star point”. All the chassis of the instrumentation, shields of cables, helium dewar and the best configuration among the three tested following ones is selected:

- the low potential of the arrays is referred to the star point potential when the sampler is installed between the “high potential” of the PJVSs and the AC source and the AC source is left floating,
- the low potential of the sampler (NI-5922) is referred to the star point potential when the sampler is installed between the “low potential” of the PJVSs and the AC source,
- the low potential of the arrays is **not** referred to the star point potential when the sampler is installed between the “high potential” of the PJVSs and the AC source and the low side of the sampler is referred to the star point potential.

In the present case, the third configuration, shown in Fig. 4, gave the best results.

4.5 Trapped flux

During the time of the comparison, it was regularly checked whether either of the two AC quantum voltmeters had trapped flux. In particular, trapping flux often appears during the preliminary 7 V RMS measurements during which each step of the measurement process is to be monitored to understand precisely when the array traps flux.

5. Comparison results - Option IV at the 0.75 V and 7 V level

5.1 Measurements at 0.75 V

At 0.75 V, the results are summarized in table 2 and on Fig. 5

***f* / Hz**	**7.8125**	**62.5**	**125**	**312.5**	**625**	**1250**
Mean / nV	-99.1	33.6	193	163	-81.0	-406
Type A unc. / nV	157	34.3	59.0	27.5	209	236

Table 2: Comparison results presented as ($U_{CENAM} - U_{BIPM}$) obtained with the Option IV of the protocol at 0.75 V RMS.

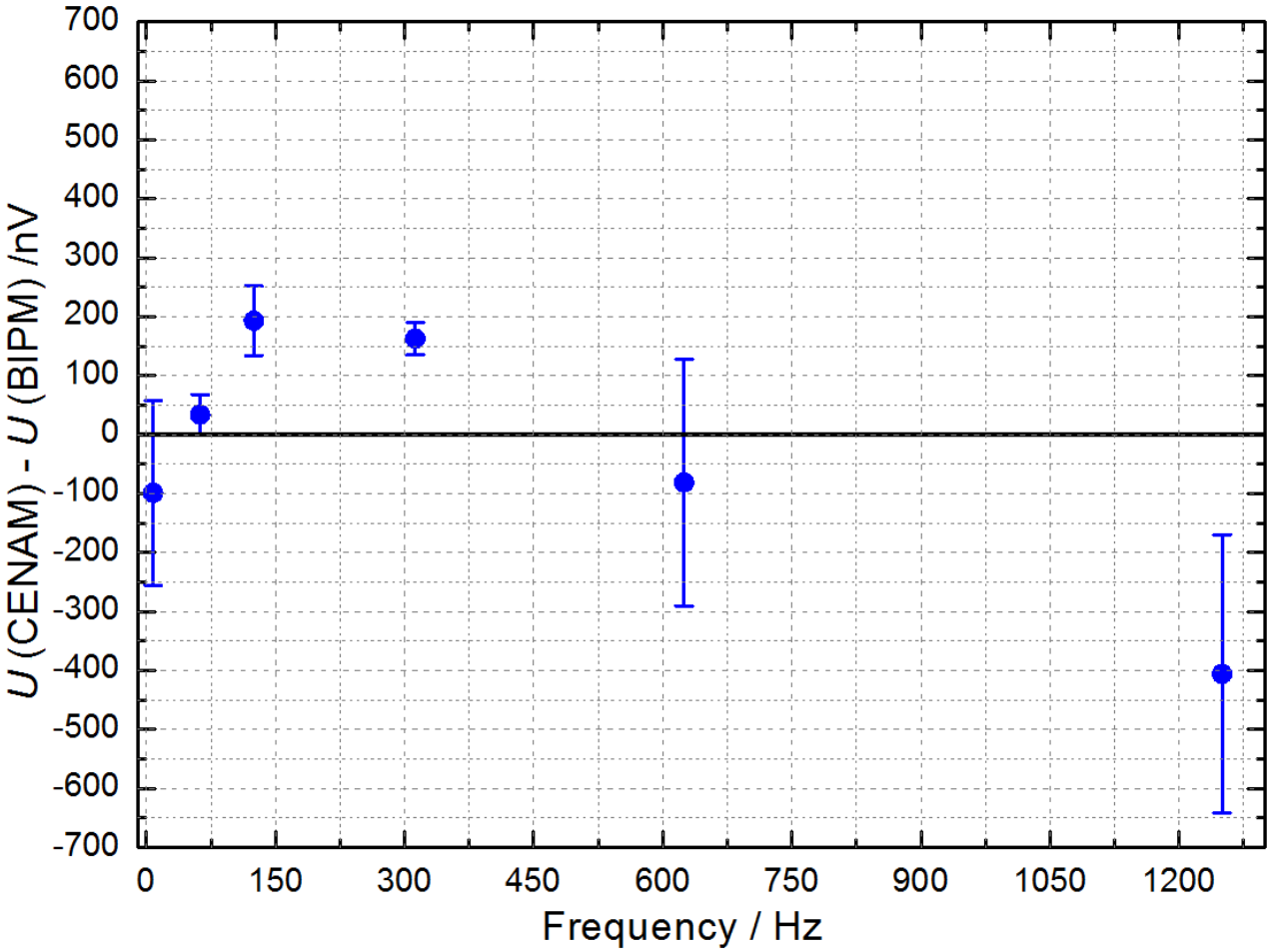

Fig. 5: Individual results obtained at 0.75 V for frequencies from 7.8125 Hz to 1.25 kHz. The uncertainty bars indicate the Type A standard uncertainty of the measurements.

The results are calculated as the mean values of the measured points applying the **ABBA** measurement scheme on different days. Details are given in the Appendix A. ($U_{CENAM} - U_{BIPM}$) is presented in nanovolts with a Type A uncertainty which is calculated as the standard deviation of the mean of all the measurements. In Figure 5, the mean comparison values for all investigated frequencies at 0.75 V RMS are presented. The uncertainty bars indicate the Type A uncertainty of the measurements for k = 1. For the Type B uncertainty evaluation see chapter 6.

It is important to note that small changes/errors in the measurement setups could lead to unforeseeable interferences leading to a poor reproducibility.

5.2 Measurements at 7 V

At 7 V RMS, only one frequency was measured and the result is presented in table 3 and on Fig. 6

***f* / Hz**	**62.5**
Mean / nV	-49.2
Type A unc. / nV	279

Table 3: Comparison results presented in absolute value as ($U_{CENAM} - U_{BIPM}$) obtained with the Option IV of the protocol at 7 V RMS at 62.5 Hz.

On 21 August, we carried out 2 series of 5 **ABBA** measurement points for the frequency 62.5 Hz. There are represented on Fig. 6 together with the Type A standard uncertainty. All the other attempts to measure the 7 V RMS sinewave at different frequencies failed as the results were unreproducible due to the electrical noise. We believe the reason relies on the fact that the He gas pipes of the CENAM cryocooler were not isolated, creating a consequent ground loop with the compressor, creating a large electrical noise on the BIPM-PJVS from time to time.

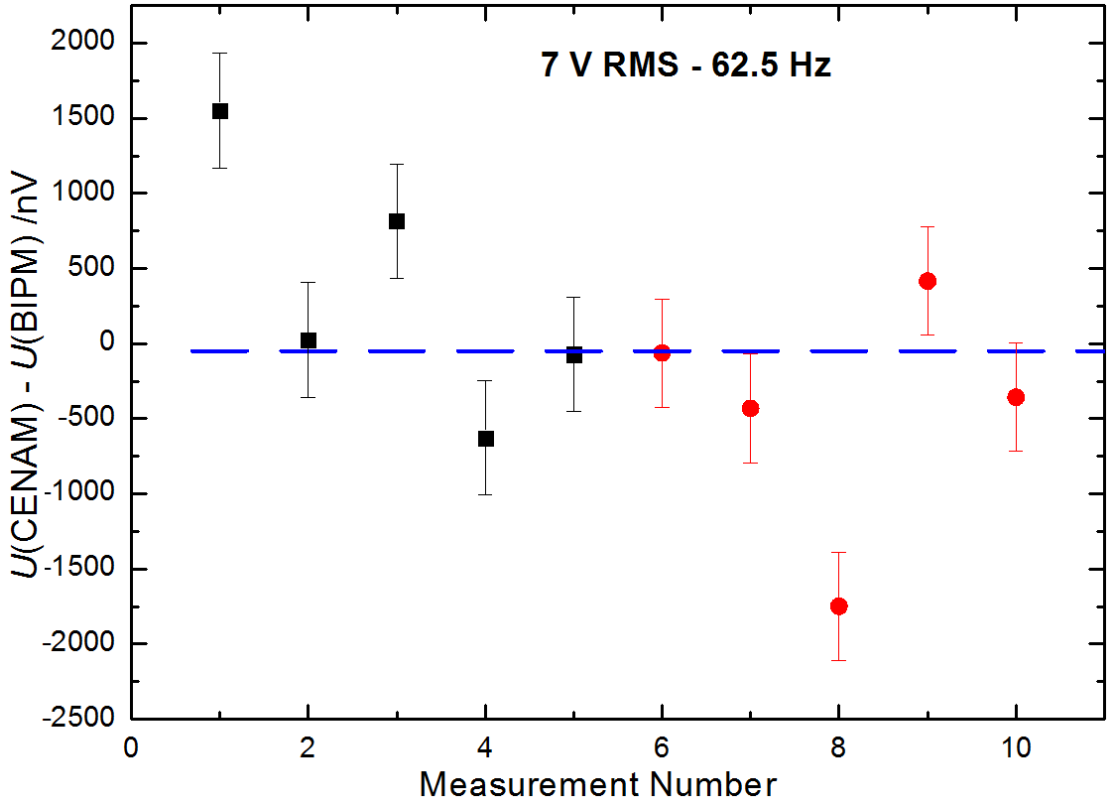

Fig. 6: Individual results obtained for two series (black square and red disks) performed at 7 V for the frequency 62.5 Hz. The uncertainty bars indicate the Type A uncertainty of the measurements for $k = 1$.

6. Evaluation of the Type B uncertainty components (option IV of the protocol)

The sources of Type B uncertainty for 0.75 V at 1.25 kHz and 7 V at 62.5 Hz (Tables 4 and 5 respectively) are: the frequency accuracy of the BIPM and the CENAM microwave synthesizers, the leakage currents, the sampler gains and filters, the cable errors, and the switch. Uncertainties which are relevant for DC Josephson voltage standards like frequency uncertainty and leakage resistance are only shown for the sake of completeness. They are irrelevant for the AC comparison, as are the thermal voltages, typically only a few 100 nV. These contribute quadratically to the effective value of the measured voltage, result normally in less than 10^{-12} volt and are therefore negligible. Most of the effects of sampler noise and gain stability are already contained in the Type A uncertainty. The effect of electromagnetic interferences is also contained in the Type A uncertainty of the measurements. Uncertainty components related to RF power rectification and sloped Shapiro voltage steps are considered negligible because no such behaviour was observed. The drift of the BIPM transfer standard was followed by each measurement setup and therefore is also part of the Type A uncertainty.

	Type	Relative uncertainty at 0.75 V and 1.25 kHz in V V^{-1}	
		BIPM	**CENAM**
Frequency offset (A)	B	3.2×10^{-12}	3.2×10^{-13}
Leakage resistance (B)	B	1.8×10^{-11}	3.3×10^{-11}
Sampler Filter (C)	B	Neglected	9.8×10^{-9}
Sampler Gain (D)	B	4.0×10^{-8}	3.5×10^{-8}
Cable error (E)	B	0.2×10^{-8}	
Switch (F)	B	1.6×10^{-8}	
CMRR (G)	B	Neglected	

Table 4: Estimated Type B relative standard uncertainty components at 0.75 V and 1.25 kHz.

	Type	Relative uncertainty at 7 V and 62.5 Hz in V V^{-1}	
		BIPM	**CENAM**
Frequency offset [A]	B	3.2×10^{-12}	3.2×10^{-13}
Leakage resistance [B]	B	1.8×10^{-11}	3.3×10^{-11}
Sampler Filter [C]	B	Neglected	9.8×10^{-9}
Sampler Gain [D]	B	4.0×10^{-8}	5.3×10^{-9}
Cable error [E]	B	2×10^{-9}	
Switch [F]	B	1.6×10^{-8}	
CMRR [G]	B	Neglected	

Table 5: Estimated Type B relative standard uncertainty components at 7 V and 62.5Hz.

[A] As both systems were locked to the same 10 MHz frequency reference, only Type B uncertainties from the frequencies of the two RF synthesizers are included. The 10 MHz signal used as the frequency reference for the comparison was produced by CENAM atomic clock.
The relative frequency uncertainty for the offset of the frequency of the BIPM PJVS can be calculated from the formula: $u_f = (1/\sqrt{3}) \times (0.1/18.3) \times 10^{-9} = 3.2 \times 10^{-12}$ in V V^{-1}.

As already mentioned, CENAM's frequency synthesis is better than 0.01 Hz. During the AC voltage comparison, a signal with a frequency of 18.24 GHz was applied to the Josephson array. We assume a rectangular statistical distribution to the value, therefore the relative uncertainty for the offset of the frequency is: $u_f = (1/\sqrt{3}) \times (0.01/18.24) \times 10^{-9} = 3.2 \times 10^{-13}$

[B] If a rectangular statistical distribution is assumed then the relative uncertainty contribution of the leakage resistance R_L and the series resistance r can be calculated as: $u_L = (1/\sqrt{3}) \times (r / R_L)$. For CENAM, the related variables were measured to be $r = 1.3\ \Omega$ and $R_L = 2.3 \times 10^{10}\ \Omega$. The isolation resistance value includes all the cables from the PJVS to the DVM. For BIPM, those parameters are measured as $r = 2.5\ \Omega$ and $R_L = 8 \times 10^{10}\ \Omega$ [16].

(C) The error due to the digital filter of the NI PXI 5922, used by the BIPM, has been investigated and published in previous papers [8,18-19]. To minimize the error as much as possible due to different filter functions the BIPM sampler was set to the 10 MSa/s sampling rates for all frequencies above 62.5 Hz and 4 MSa/s at 62.5 Hz always using the “48-tap standard” finite-impulse-response digital filter. We assume that small errors at these low frequencies can be completely neglected.

The Fluke 8588A multimeter, when operated as a digitizer on all ranges, incorporates a selectable analog input filter (100 kHz, 3 MHz, or bypass) located before the analog-to-digital converter (ADC) [20]. In the quantum voltmeter measurements performed at CENAM, the instrument is used on the 1 V range with the 3 MHz filter enabled.

The system operates as a quantum voltmeter through differential comparison between a sinusoidal signal and the output of a Programmable Josephson Voltage Standard (PJVS). The processing relies on windowed averaging positioned exclusively within the stable region of each PJVS step, deliberately avoiding the transients associated with level transitions.

Under these conditions, the analog filter preceding the ADC does not modify the nominal amplitude of the sinusoidal signal, but only the difference signal. The relevant spectral content of this signal is concentrated at low frequencies, mainly at DC and at the fundamental frequency of the sinusoid, a region in which the magnitude response of the filter is practically unity.

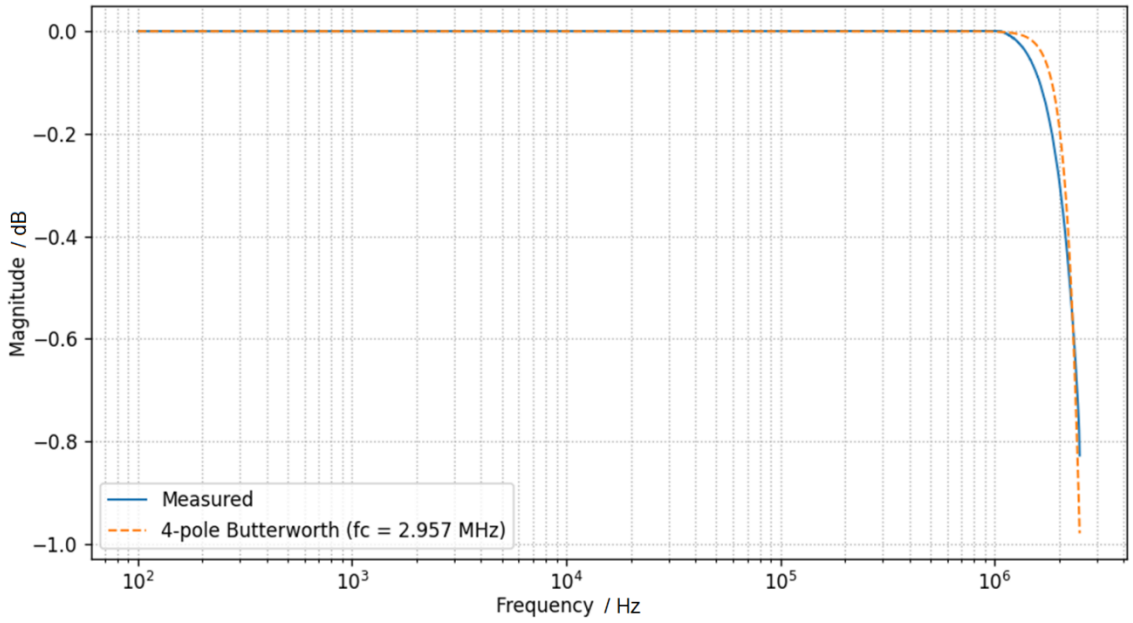

Fig. 7. Measured magnitude response of the analog input filter of the Fluke 8588A on the 1 V range and its approximation using a fourth-order Butterworth filter.

The measured filter response is approximated by a fourth-order Butterworth low-pass model, whose magnitude is expressed as:

$$| H(f) | = \frac{1}{\sqrt{1 + (f/f_c)^8}},$$

where f_c is the cutoff frequency obtained from a fit to the experimental data. The model adequately reproduces the filter response within the frequency band of interest (cf. Fig.7).

Numerical simulations were performed to quantitatively estimate the effect of the filter on differential sampling when measuring an ideal sinusoidal waveform $V(t)$. Assuming a PJVS waveform $V_J(t)$ with the same frequency as $V(t)$, the differential signal is defined as:

$$\Delta V_0(t) = V(t) - V_J(t).$$

The differential signal in the frequency domain, $\Delta V_0(f)$, was obtained using a discrete Fourier transform (DFT). Applying the filter transfer function $H(f)$, modeled as a four-pole filter,

$$\Delta V_{\mathrm{flt}}(f) = \Delta V_0(f)\, H(f),$$

and performing the inverse transform yields $\Delta V_{\mathrm{flt}}(t)$.

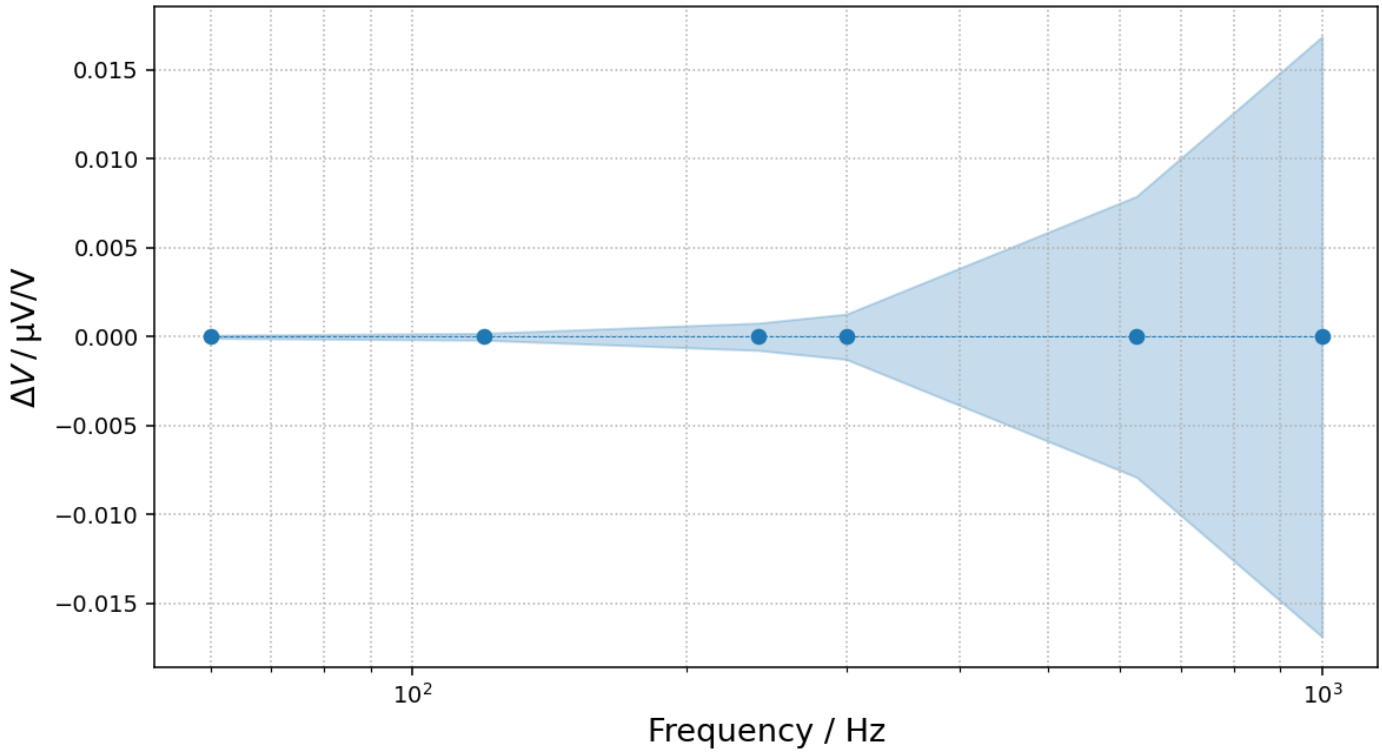

Fig. 8. Sensitivity of reconstructed RMS voltage to gain variation (ΔG = ±10 ppm). The blue dots correspond to the simulated values at each frequency point, and the shaded area represents the envelope of the results obtained for both polarities of ΔG.

To conservatively estimate the impact of the filter correction on the measurement results, a relative variation ΔG was applied to the gain G of the transfer function, where ΔG represents a perturbation of ±10 ppm.

A numerical simulation was then performed to evaluate the effect of this variation on the reconstructed RMS voltage. The resulting variation is expressed as

$\Delta V = V_{(G-\Delta G)} - V_{(G+\Delta G)}$, which represents the differential effect between both gain perturbation polarities.

The results of the simulation are shown in Fig. 8, where the vertical axis corresponds to ΔV and the frequency dependence of the effect is evaluated. The blue dots represent the simulated values at each frequency point, while the shaded area represents the envelope of the results obtained for both polarities of ΔG.

The result shows that at 1 kHz this variation produces a change of ±0.017 μV/V in the reconstruction of the RMS value. Consequently, the uncertainty contribution is estimated as:

$$u = \frac{0.017\ \mu\text{V/V}}{\sqrt{3}} = 9.8 \times 10^{-9}\ \text{V V}^{-1}$$

which is assigned as the uncertainty component associated with the filter function.

(D) The sampler gain was usually calibrated before each new **ABBA** measurement series using a triangle approximated waveform generated by each PJVS matching the maximum voltage difference measured by the sampler. The PJVS peak amplitude was set to 150 mV (for 0.75 V) and 1 V (for 7 V), i.e. the expected amplitudes at the sampler in the differential measurement. Then, for differential sampling the PJVS peak amplitude was set to 1.0606 V (for 0.75 V RMS), we synchronized the two systems and measured the SWG RMS amplitude with the AC-QVM. Each measurement point is adjusted by its corresponding gain and offset values.
The software used to reconstruct the waveform at the input of the AC-QVM includes the gain of the sampler as a parameter. The gain of the BIPM-5922 was regularly measured all along the comparison and varied by 10 μV V^{-1} at most. To determine the influence of the gain variation, we deliberately changed the gain by ± 1000 μV V^{-1}. The corresponding changes in the amplitude are suppressed for differential sampling with 16 Josephson steps with the BIPM setup by a factor of 253.Considering a gaussian distribution the relative uncertainty is u_G = 10 μV V^{-1} / 253 = 3.95 × 10^{-8} V V^{-1} (k = 1).

The same approach was employed to determine the gain correction of the CENAM sampler. The PJVS-CENAM peak amplitude was set to 200 mV and 1 V, values consistent with the differential measurement conditions of the alternating-current quantum voltmeter (AC-QVM) at CENAM.
The software developed at CENAM for AC measurements incorporates the sampler gain as a correction parameter. The gain calibration of the Fluke 8588A digitizer was carried out using the 1 V range and a 3 MHz analog filter, by measuring a triangular waveform. Subsequently, for differential sampling, the PJVS peak amplitude was set to 1.0606 V (corresponding to 0.75 V RMS) and to 9.8994 V (corresponding to 7 V RMS). Both systems were synchronized, and the SWG RMS was measured using the AC-QVM. Each measurement point was corrected using its corresponding gain value.
The gain of the Fluke 8588A was periodically monitored throughout the comparison and exhibited variations of up to 40 μV V^{-1}; similar levels of variation were also observed at NIST using the JAWS [21]. To evaluate the influence of these variations, the software that reconstructs the waveform at the input of the AC-QVM was modified, and the gain was deliberately varied by ±100 μV V^{-1}. The resulting changes in the reconstructed RMS voltage, denoted as ΔU, were

evaluated for an effective gain variation of ±40 µV V⁻¹, yielding changes of 45.3 nV at 0.75 V RMS and 64 nV at 7 V RMS, as shown in figure 9.

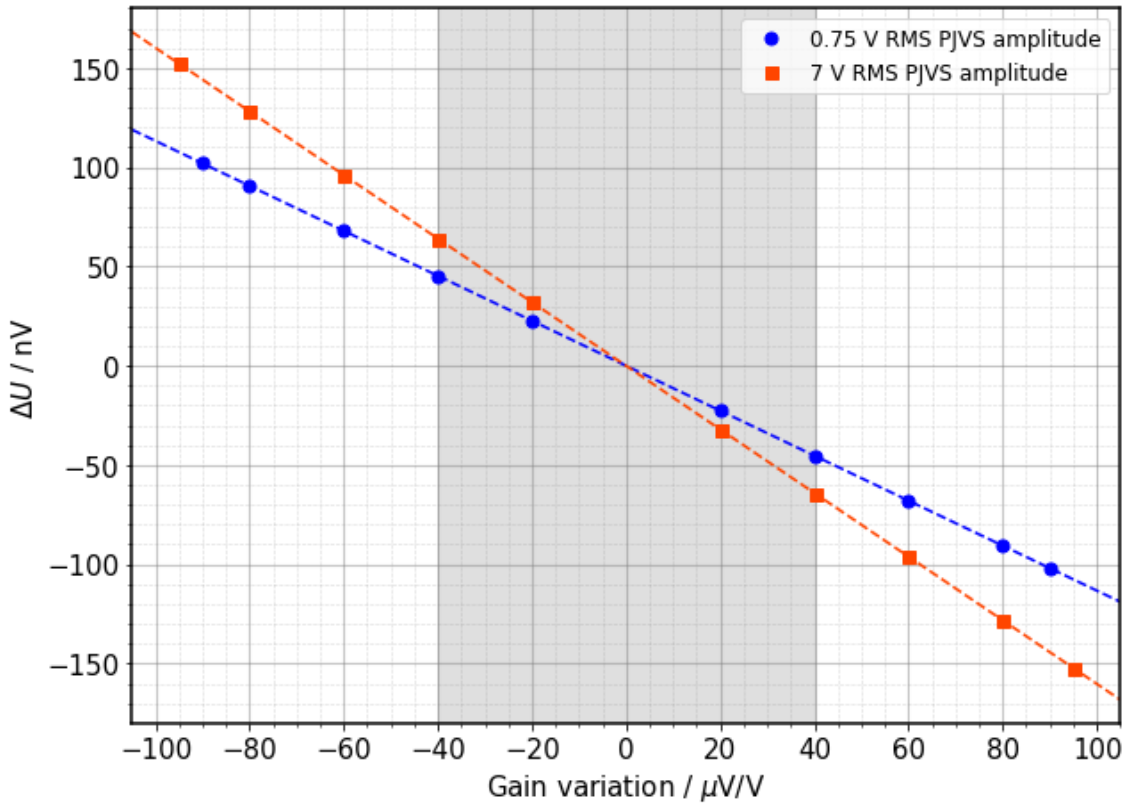

Fig. 9. Sensitivity of the reconstructed RMS voltage ΔU to gain variation in the CENAM sampler (Fluke 8588A). Results are shown for PJVS amplitudes of 0.75 V RMS and 7 V RMS. The shaded region corresponds to the experimentally observed gain variation range (±40 µV V⁻ ¹)..

Assuming a rectangular distribution for the uncertainty contribution associated with the gain, the corresponding uncertainties are, with a coverage factor $k = 1$:

$$u_{G1} = \frac{45\ \text{nV}}{\sqrt{3}} = 2.6 \times 10^{-8}\ \text{V},$$

$$u_{G2} = \frac{64\ \text{nV}}{\sqrt{3}} = 3.7 \times 10^{-8}\ \text{V},$$

(E) The Josephson voltages are only quantised on the chip. Due to the long output cables, the AC voltages at the sampler have an error. At 1 kHz, the relative error is approximately 3 x 10^{-8} V V^{-1}. As the BIPM and CENAM Josephson voltage standards use approximately the same cable lengths and different cables, the differences are difficult to estimate. In addition, the current source also

has an influence on the cable error. Only the difference between the two cable errors needs to be considered for the comparison and is known to lead to very small changes in the comparison result. Because cable lengths contribute quadratically to the error, a quadratic fit can describe the observed deviations with cable extensions as described in pages 12 and 13 of the PTB-BIPM comparison report [22]. The cable error is estimated to 0.2×10^{-8} V V^{-1} (k = 1).

(F) The contribution from the switch was evaluated experimentally by performing two consecutive measurements immediately before and after interchanging the inputs used by the PJVS systems. The differences between *Forward* and *Reversed* measurements were -1.7×10^{-8} V V^{-1} and 7.2×10^{-8} V V^{-1} for the BIPM and CENAM, respectively. From this, we evaluate the measurement uncertainty for the switch as

$$((7.2 - 1.7)\ \text{V V}^{-1} \times 10^{-8}\ /2)\ / \sqrt{3} = 1.59 \times 10^{-8}\ \text{V V}^{-1}\ (k = 1).$$

(G) The common mode rejection ratio (CMRR) of the sampler contributes to the measured value for the measurements at 7 V and only the difference in CMRR between the two samplers employed affects the result of the comparison. For all the measurements performed at 0.75 V RMS, we can neglect this uncertainty. There is only one frequency investigated at 7 V: 62.5 Hz, and the CMRR wasn't measured during the comparison.

However, at 7 V RMS and 62.5 Hz, the BIPM carried out 3 series of measurements using each of the 3 samplers one after the other (cf. Fig 10). The Type A uncertainty of the nine measurements is 2.83×10^{-8} which is half the dispersion of each series. From this, it can be considered that the CMRR is not a major contribution in the dispersion of the results when using different samplers with the BIPM PJVS and therefore can be neglected for this particular measurement.

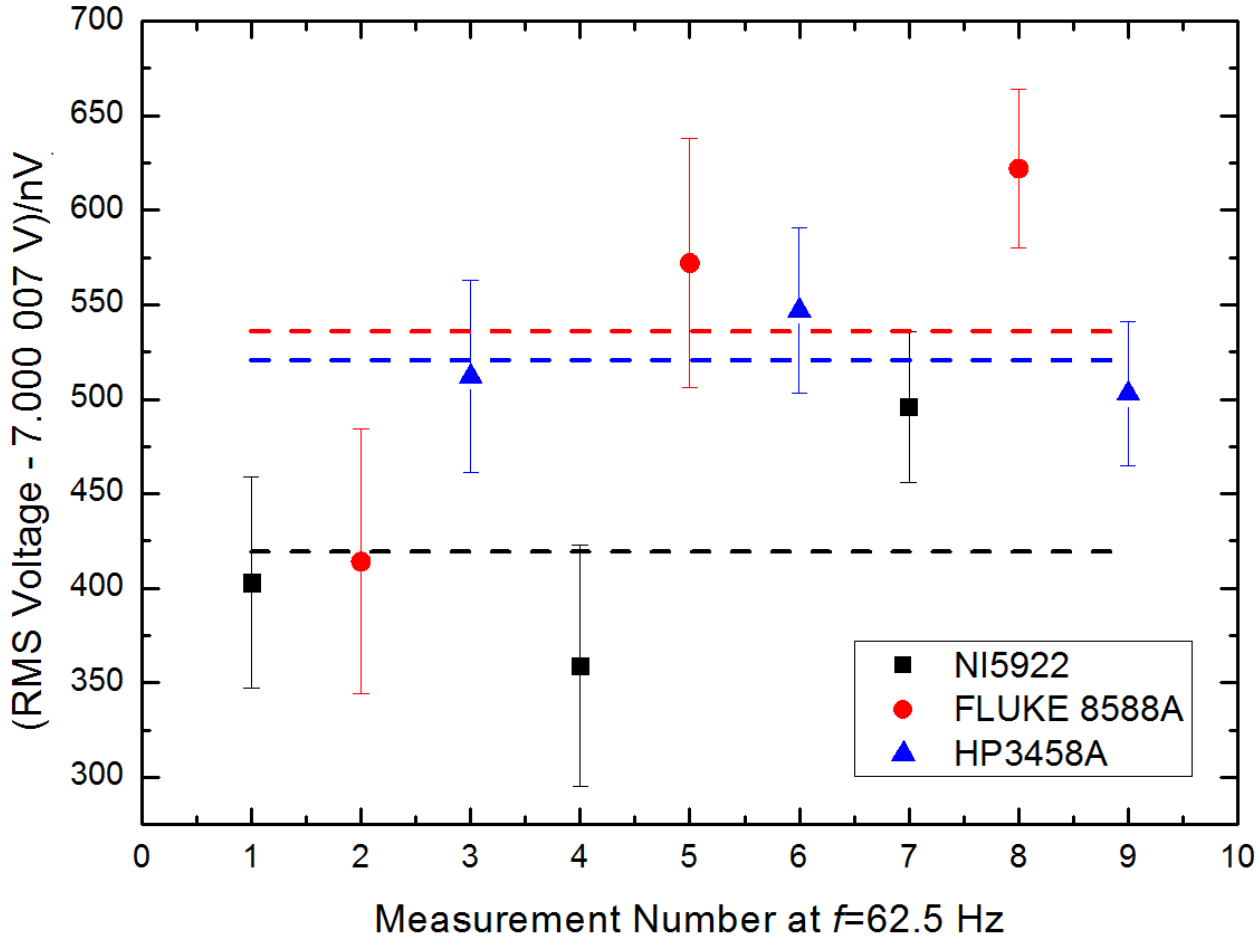

Fig. 10: Individual results obtained for three series performed at 7 V for the frequency 62.5 Hz using the 3 BIPM samplers. (The uncertainty bars indicate the Type A uncertainty of the measurements for $k = 1$). The dashed lines are the average of the three points with respect to the color of the individual points.

For the option IV comparison protocol, the total combined Type B uncertainties comprise all the BIPM Type B components to which the CENAM Type B uncertainties are combined quadratically:

$u_{B\ (option\ IV)} / U_{BIPM} = 5.6 \times 10^{-8}$ V V^{-1} at 0.75 V – 1.25 kHz and $u_{B\ (option\ IV)} / U_{BIPM} = 4.4 \times 10^{-8}$ V V^{-1} at 7 V and 62.5 Hz.

7. Conclusion of Option II of the protocol

This BIPM.EM-K10 comparison was carried out in the CENAM Electricity Laboratories in Querétaro where the environmental conditions allowed meeting excellent conditions for the stability of the quantum voltages. The CENAM DC Quantum Voltage Standard was compared to the BIPM Transportable PJVS at 1 V and 10 V: an excellent agreement was found at the two nominal voltages. The degrees of equivalence are defined as the relative voltage difference $(U_{CENAM} - U_{BIPM}) / U_{BIPM}$ together with the corresponding relative combined standard uncertainty u_c / U_{BIPM} where U_{CENAM} is the CENAM measured voltage, U_{BIPM} is the BIPM measured voltage *and* u_c is the combined standard uncertainty with a coverage factor of $k = 1$.

Nominal Voltage /V	1	10
Relative Difference / 10^{-11}	-57	+3.6
Relative Total Combined Uncertainty / 10^{-11}	87	8.0

Degrees of equivalence CENAM - BIPM for the DC comparison at 1 V and 10 V.

8. Conclusion of Option IV of the protocol

The CENAM AC Quantum Voltmeter was compared to the BIPM Quantum Voltage Standard. This is the second comparison of this kind since the BIPM.EM-K10 comparison protocol has been revised and extended to measurements of AC voltages using the differential sampling technique. Despite several pilot studies performed in preparation it is still a difficult exercise in particular because of the introduction of several possible systematic errors [17, 22]. For example, it was not easy to avoid interferences caused by small inaccuracies in the measurement setup. These interferences can lead to significant deviations of the order of a few 10^{-7} V V^{-1}. In addition, the fact that the housing of the He pipes of the CENAM cryocooler was not isolated from the Earth potential brought significant electrical noise and created a significant ground loop.

Further investigations should be carried out in this field, especially on the determination of the Type B uncertainties, and particularly the capacitive component of the leakage impedance to ground. A pilot study operating the NIST Josephson Arbitrary Waveform Synthesizer and the BIPM-PJVS in 2024 demonstrated that a systematic error of up to 100 nV can be reached at 1000 Hz due to AC leakages for AC voltage levels comprised between 0.75 V RMS and 1.5 V RMS.

The electromagnetic compatibility of the participant laboratory as well as the quality of the mains power have also a strong impact on the quality of the measurements and are very difficult to quantify.

Despite these main difficulties, the BIPM PJVS travelling standard and CENAM Quantum Voltmeter were successfully compared to a relative agreement of a few parts in 10^8 for both voltages (0.75 V RMS and 7 V RMS) at 62.5 Hz and a few parts in 10^7 for 0.75 V RMS for larger frequencies up to 1250 Hz. The degrees of equivalence are reminded in the following tables as:

The relative voltage difference ($U_{CENAM} - U_{BIPM}$) / U_{BIPM} together with the corresponding relative combined standard uncertainty u_c / U_{BIPM} where U_{CENAM} is the CENAM measured voltage, U_{BIPM} is the BIPM measured voltage *and* u_c is the combined standard uncertainty with a coverage factor of k = 1.

Frequency / Hz	7.8125	62.5	125	312.5	625	1250
Relative Difference / 10^{-8}	-13	4.5	26	22	-11	-54
Relative Combined Uncertainty / 10^{-8}	21.7	7.3	9.7	6.7	28.4	32

Degrees of equivalence CENAM - BIPM for the comparison at 0.75 V RMS.

Frequency / Hz	62.5
Relative Difference / 10^{-9}	-7.0
Relative Combined Uncertainty / 10^{-8}	6.0

Degree of equivalence CENAM - BIPM for the comparison at 7 V RMS and 62.5 Hz.

References

[1] Solve S 2023 On-site comparison of dc and ac voltages from Josephson arrays Technical Protocol for BIPM.EM-K10 comparisons, BIPM KCDB https://www.bipm.org/kcdb/comparison?id=1779

[2] Behr R, Palafox L, Ramm G, Moser H, and Melcher J 2007 Direct comparison of Josephson waveforms using an AC quantum voltmeter *IEEE Transactions on Instrumentation and Measurement* 56 pp 235–8 https://doi.org/10.1109/TIM.2007.891076

[3] Rüfenacht A, Burroughs C J, Dresselhaus P D, and Benz S P 2013 Differential sampling measurement of a 7 V RMS sine wave with a programmable Josephson voltage standard *IEEE Transactions on Instrumentation and Measurement* 62 pp 1587–93 https://doi.org/10.1109/TIM.2013.2237993

[4] Lee J, Behr R, Palafox L, Katkov A, Schubert M, Starkloff M and Böck A C 2013 An AC quantum voltmeter based on a 10 V programmable Josephson array *Metrologia* 50 pp 612–22 https://doi.org/10.1088/0026-1394/50/6/612

[5] Rufenacht A, Burroughs C J, Benz S P, Dresselhaus P D, Waltrip B C and Nelson T L 2009 Precision Differential Sampling Measurements of Low-Frequency Synthesized Sine Waves With an AC Programmable Josephson Voltage Standard *IEEE Transactions on Instrumentation Measurement* pp 70-1 https://doi.org/10.1109/TIM.2008.2008087

[6] Kleinschmidt P, Patel P D, Williams J M and Janssen T J B M 2002 Investigation of binary Josephson arrays for arbitrary waveform synthesis *IEE Proc.-Sci. Meas. Technol.* 49 313–6

[7] Kim M-S, Cho H, Chayramy R and Solve S 2020 Measurement configurations for differential sampling of AC waveforms based on a programmable Josephson voltage standard: effects of sampler bandwidth on the measurements *Metrologia* 57 065020 https://doi.org/10.1088/1681-7575/aba040

[8] Kim M-S, Cho H, Chayramy R, Solve S 2025 Effect of Sampler Characteristics in Differential Sampling Adopting a Programmable Josephson Voltage Standard *IEEE Transactions on Instrumentation and Measurement* 74 1501507 https://doi.org/10.1109/TIM.2025.3544691

[9] Burroughs C J, Rufenacht A, Benz S P, Dresselhaus P D, Waltrip B C and Nelson T L 2008 Error and Transient Analysis of Stepwise-Approximated Sine Waves Generated by Programmable Josephson Voltage Standards *IEEE Transactions on Instrumentation and Measurement,* https://doi.org/10.1109/TIM.2008.917260

[10] Burroughs C J, Rufenacht A, Benz S P and Dresselhaus P D 2009 Systematic Error Analysis of Stepwise-Approximated AC Waveforms Generated by Programmable Josephson Voltage Standards *IEEE Transactions on Instrumentation Measurement,* https://doi.org/10.1109/TIM.2008.2007041

[11] Burroughs C J, Dresselhaus P D, Rüfenacht A, Olaya D, Elsbury M M, Tang Y and Benz S P 2011 NIST 10 V programmable Josephson voltage standard system *IEEE Transactions on Instrumentation and Measurement* 60 pp 2482–8 https://doi.org/10.1109/TIM.2010.2101191

[12] Fox A E, Dresselhaus P D, Rüfenacht A, Sanders A and Benz S P 2015 Junction yield analysis for 10 V programmable Josephson voltage standard devices *IEEE Transactions on Applied Superconductivity* 25 pp 1–5 https://doi.org/10.1109/TASC.2014.2377744

[13] National Institute of Standards & Technology 2019 Specifications of Standard Reference Instrument Series 6000: Programmable Josephson Voltage Standard

[14] Kučera J, Kováč J, Palafox L, Behr R and Vojáčková L 2020 Characterization of a precision modular sinewave generator *Measurement Science and Technology* 31 pp 064002 https://dx.doi.org/10.1088/1361-6501/ab6f2e

[15] Avilés C D, Medina J and Navarrete E, "The CENAM Programmable Josephson Voltage Standard," 29th Conference on Precision Electromagnetic Measurements (CPEM 2014), Rio de Janeiro, Brazil, 2014, pp. 528-529, https://doi.org 10.1109/CPEM.2014.6898492.

[16] Avilés, E Navarrete and D Hernández, Comparison of the Josephson voltage standards of the CENAM and the BIPM (part of the ongoing BIPM key comparison BIPM.EM-K10.b), *Metrologia* 2012 **4**, *Tech. Suppl.* 01011 https://doi.org/10.1088/0026-1394/49/1A/01011

[17] Rufenacht A, Burroughs C J, Dresselhaus P D and Benz S P, "Measurement of Leakage Current to Ground in Programmable Josephson Voltage Standards," 2018 Conference on Precision Electromagnetic Measurements (CPEM 2018), Paris, France, 2018, pp. 1-2, Doi: 10.1109/CPEM.2018.8500911

[18] Behr R and Palafox L 2021 An AC quantum voltmeter for frequencies up to 100 kHz using sub-sampling *Metrologia* 58 025010 https://doi.org/10.1088/1681-7575/abe453

[19] National Instruments, *NI PXI/PCI-5922 Specifications: Flexible-resolution Digitizer*, Sep. 2018. http://www.ni.com/pdf/manuals/374033b.pdf

[20] Fluke 8588A Reference Multimeter *Specifications* https://media.fluke.com/519c6b95-99c3-4d1f-96ec-b1090050a96a_original%20file.pdf[

[21] Jesus Medina Mejia, Alain Rüfenacht, Raegan Johnson-Wilke, Anna E. Fox, Nathan E. Flowers-Jacobs, Sam P. Benz, and Paul D. Dresselhaus, "Digitizer Linearity Measurement with a Josephson Arbitrary Waveform Synthesizer," *2024 Conference on Precision Electromagnetic Measurements (CPEM)*, Denver, CO, USA, 2024, pp. 1-2, doi: 10.1109/CPEM61406.2024.10646120.

[22] Solve S., Chayramy R, Stock M, Behr R and Palafox L, Bilateral Comparison of AC Programmable Josephson Voltage Standard (0.75 V RMS and 7 V RMS) between the PTB (Germany) and the BIPM, June 2025 (part of the ongoing BIPM key comparison BIPM.EM-K10.c and d) Metrologia, 62 1A https://doi.org/10.1088/0026-1394/62/1A/01012

Appendix A

This appendix describes additional measurements and analyses performed.

A1: Graphs showing ABBA series for the evaluated voltages and frequencies

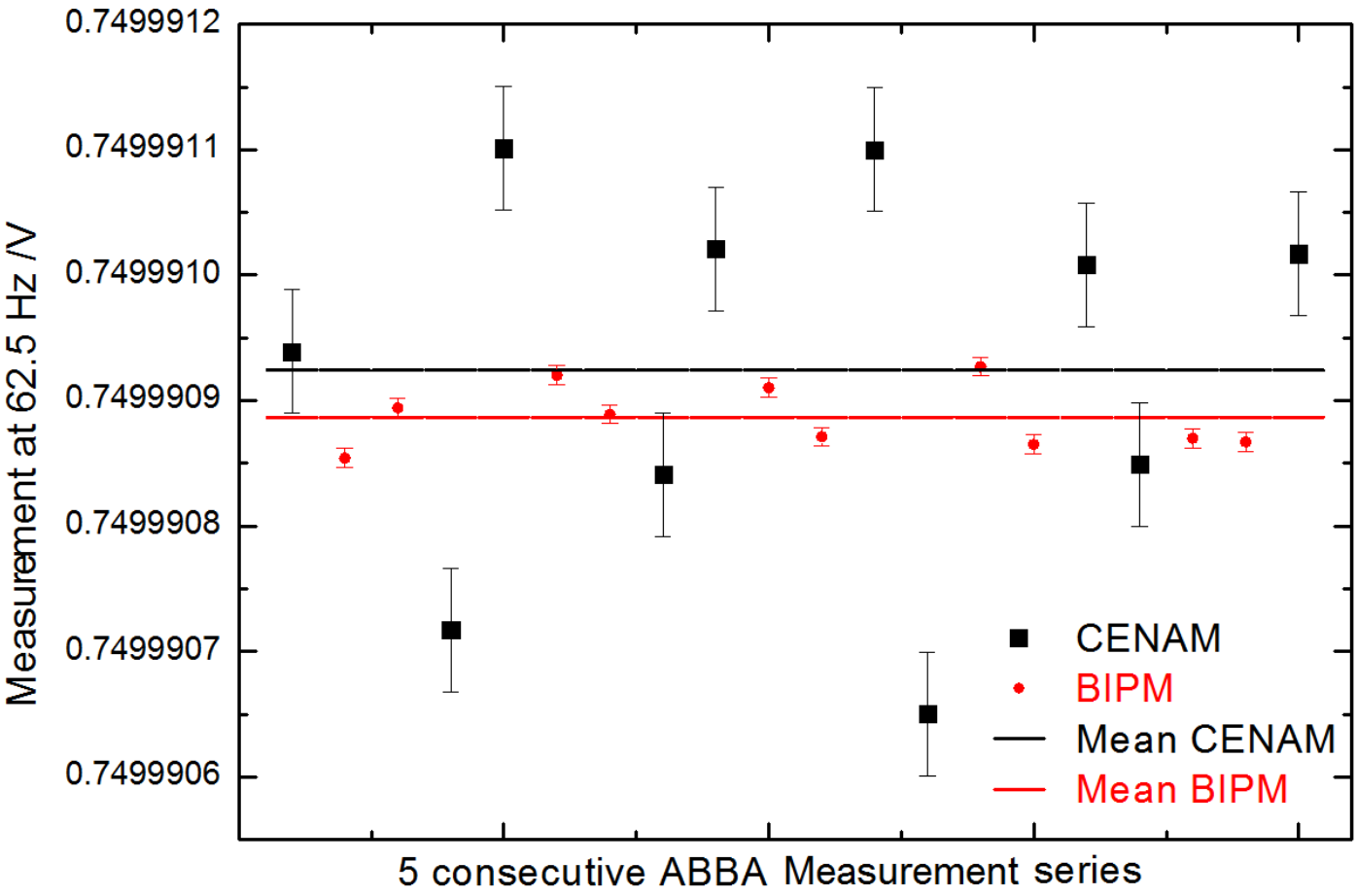

Fig. A1.1: ABBA measurement series at 0.75 V RMS and 62.5 Hz

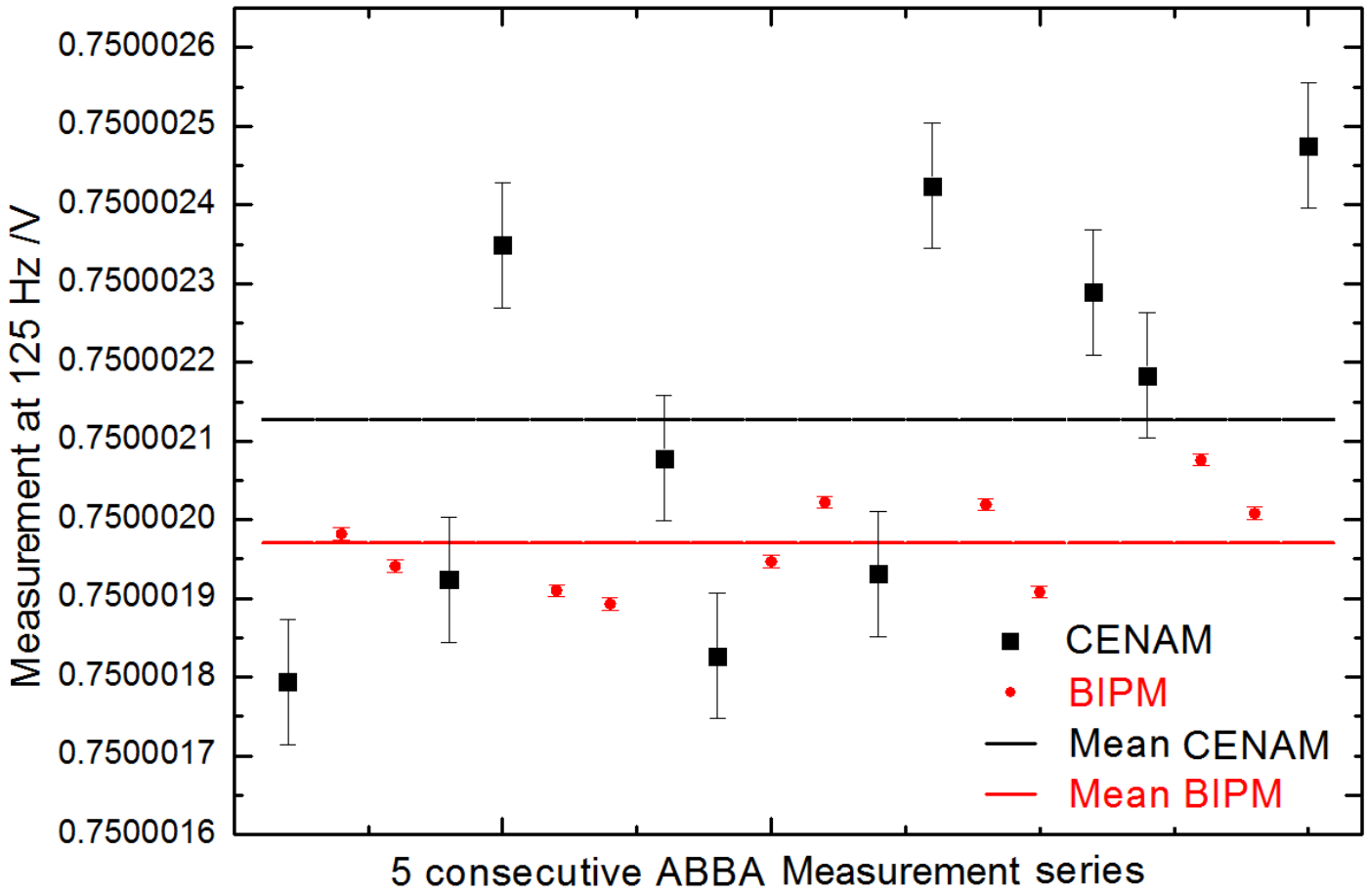

Fig. A1.2: ABBA series at 0.75 V RMS and 125 Hz

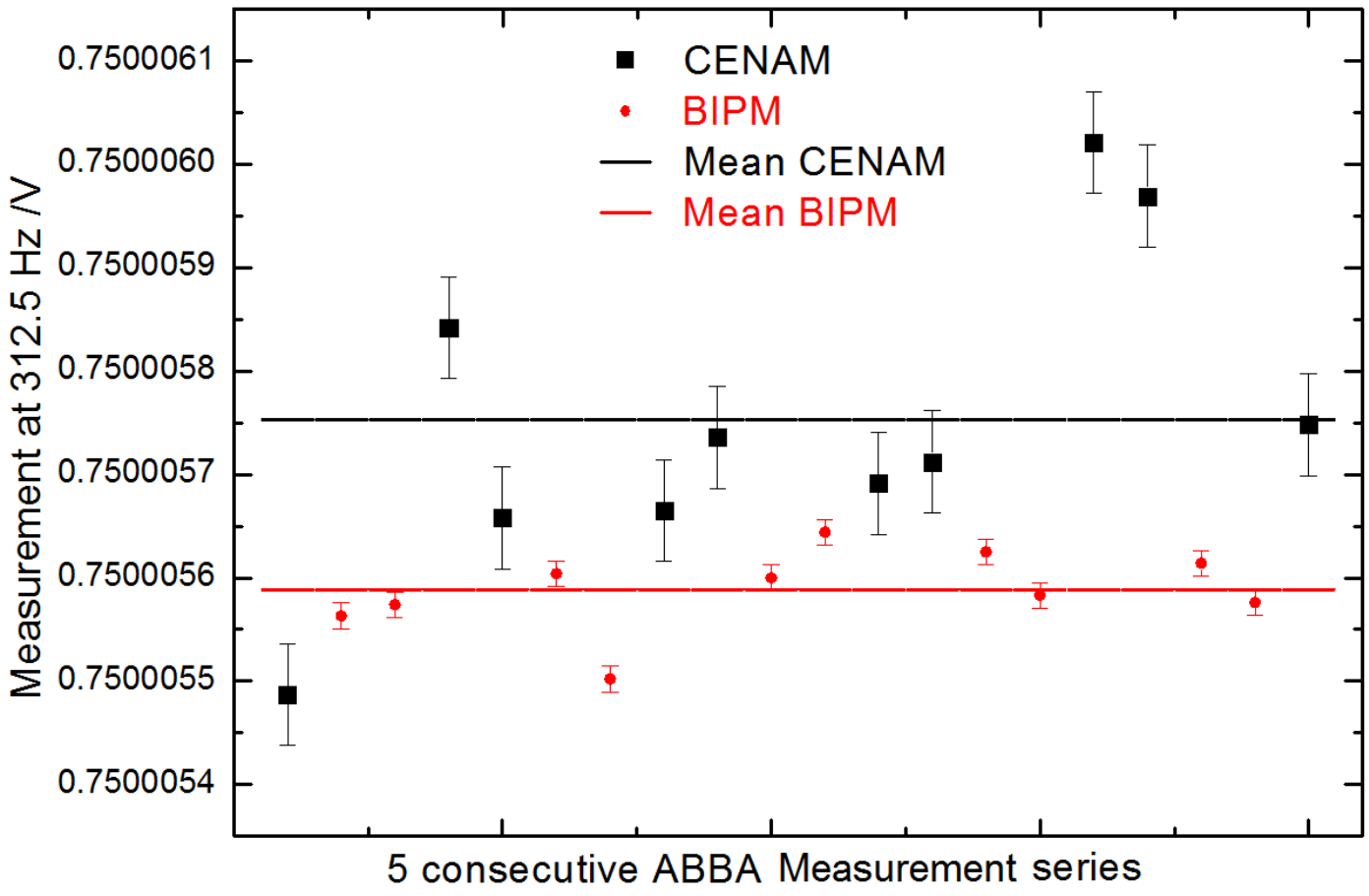

Fig. A1.3: ABBA series at 0.75 V RMS and 312.5 Hz

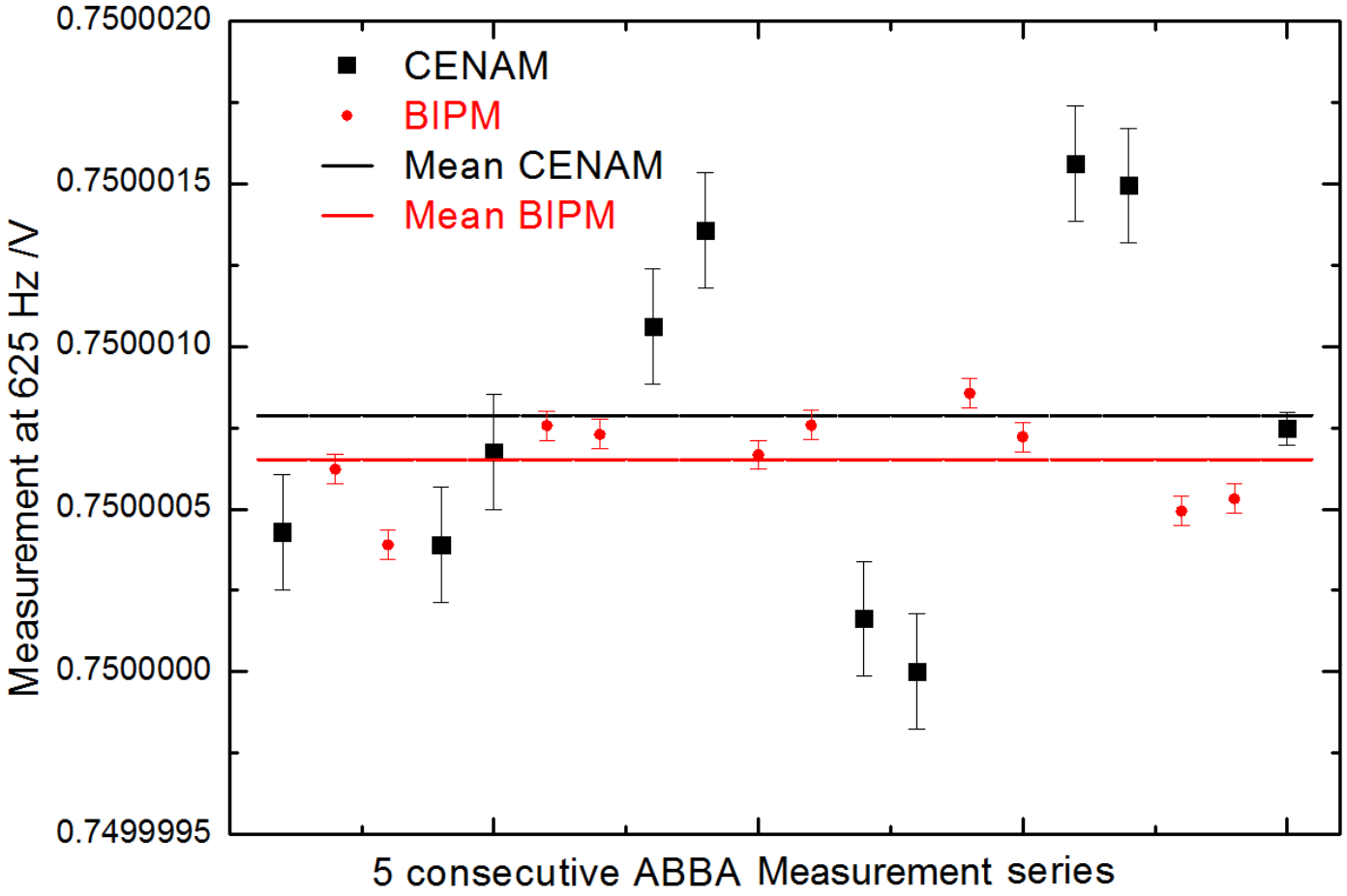

Fig. A1.4: ABBA series at 0.75 V RMS and 625 Hz

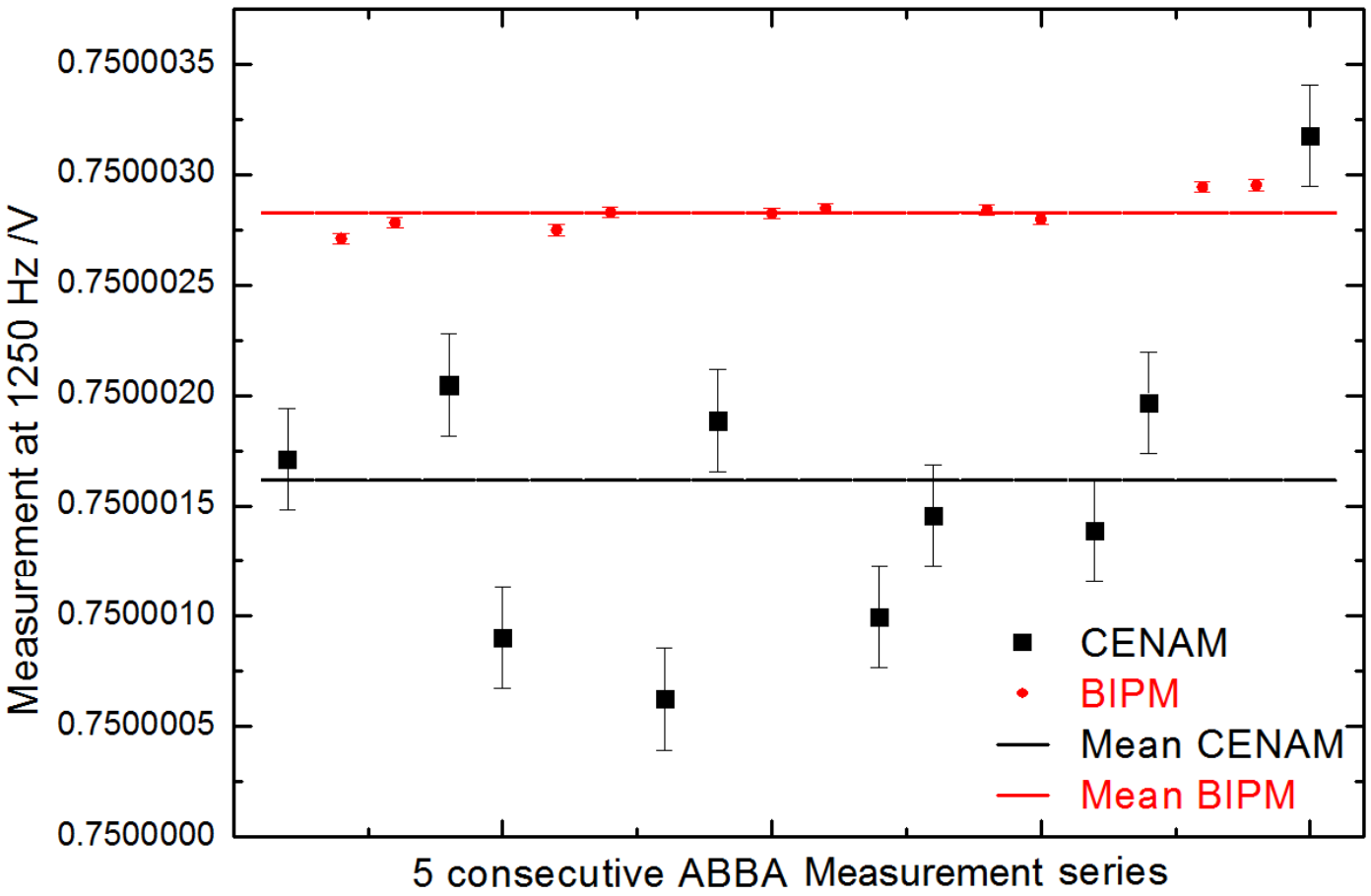

Fig. A1.5: ABBA series at 0.75 V RMS and 1250 Hz

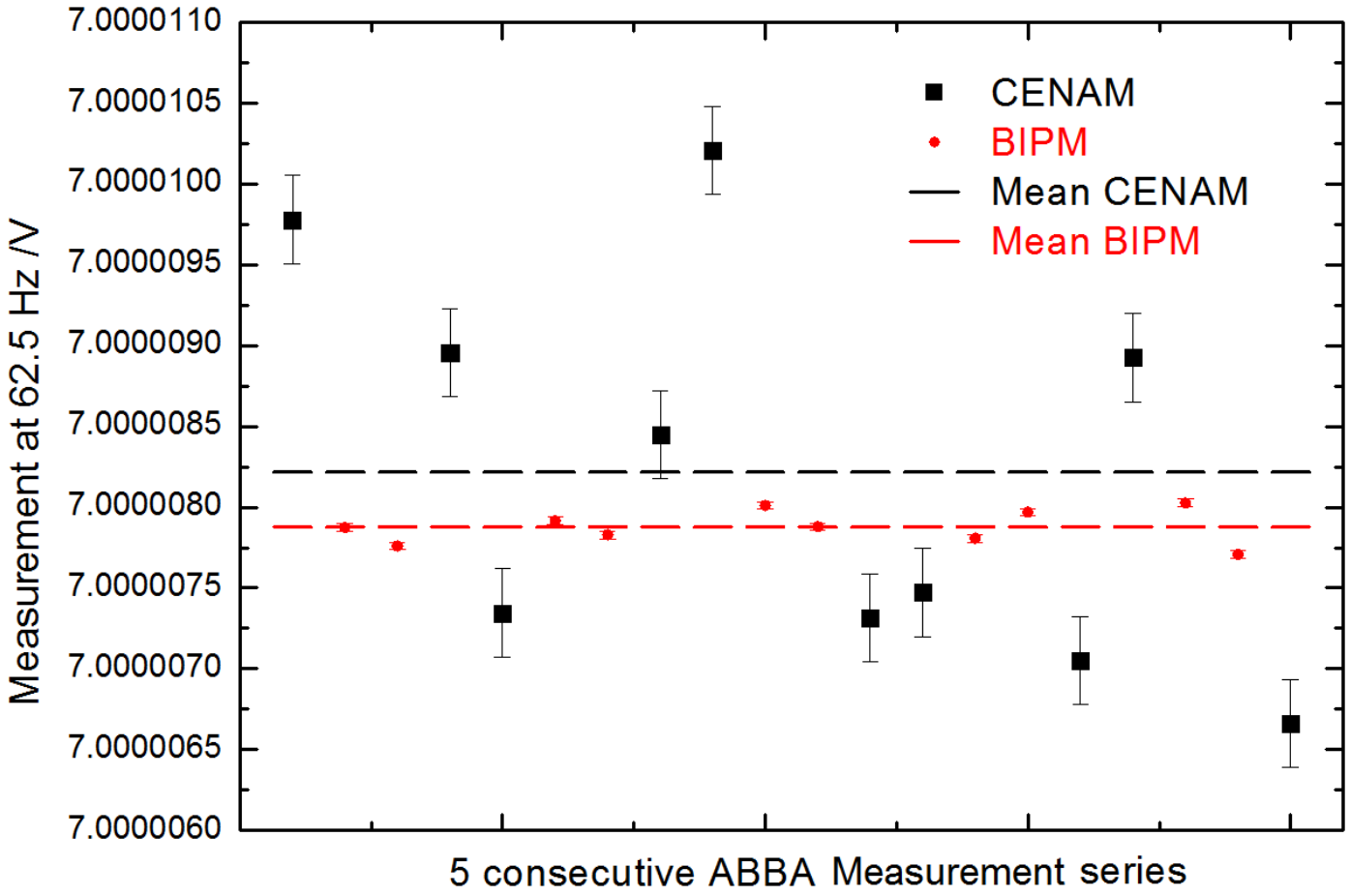

Fig. A1.6: ABBA series at 7 V RMS and 62.5 Hz